Biosensors and Bioelectronics 33 (2012) 184–189

Contents lists available at SciVerse ScienceDirect

Biosensors and Bioelectronics

journal homepage: www.elsevier.com/locate/bios

Design and construction of a label free aptasensor for electrochemical detection of sodium diclofenac

Leila Kashefi-Kheyrabadi, Masoud A. Mehrgardi*

Department of Chemistry, University of Isfahan, Isfahan, 81746-73441, Iran

ARTICLE INFO

Article history:
Received 28 September 2011
Received in revised form 5 December 2011
Accepted 25 December 2011
Available online 3 January 2012

Keywords:
Sodium diclofenac
Aptasensor
Electrochemical impedance spectroscopy
Surface plasmon band
Silver nanoparticle

ABSTRACT

The present manuscript describes a label free electrochemical aptasensor for the detection of sodium diclofenac (DCF). In order to construct the biosensor, the amino-functionalized diclofenac binding aptamer (DBA) was covalently immobilized on the surface of the glassy carbon electrode (GCE). The conformation of the DBAs on the surface of the electrode is changed when this is exposed to different concentrations of DCF. The introduction of DCF induces an alteration in the conformation of the surface immobilized DBA and causes a decrease in the charge transfer resistance of the aptasensor. However, the charge transfer resistance is increased by incubation of GCE/DBA/DCF in the secondary DBA. The changes in the charge transfer resistance have been monitored using the voltammetric and electrochemical impedance spectroscopic (EIS) techniques. The aptasensor shows two different linear dynamic ranges over 0–5.0 μM and 10 μM to 1 mM, and the sensitivity of 15.7 kΩ μM^{-1} and detection limit of 2.7×10^{-7} M were obtained. The validity of the method and applicability of the aptasensor were successfully evaluated by detection of DCF in a blood serum sample without interference from the sample matrix. Furthermore, the aptasensor has shown good stability.

© 2012 Elsevier B.V. All rights reserved.

1. Introduction

As it is well known, aptamers (artificial nucleic acids ligands) are short single-stranded DNA or RNA oligonucleotides that can bind with high affinity and specificity to a wide variety of target molecules including proteins, enzymes, antigens, antibiotics, toxins, and pharmaceutical drugs. The selection of the aptamers for different ligands was independently discovered by three laboratories in 1990 (Tuerk and Gold, 1990; Roberston and Joyce, 1990; Ellington and Szostak, 1990). The methodology for the synthesis of these aptamers is based on an in-vitro automated selection process which is called SELEX (Systematic Evolution of Ligands by Exponential enrichment) (Tuerk and Gold, 1990; Ellington and Szostak, 1990).

Aptamers have drawn considerable attention as significant recognition elements for the construction of various kinds of biosensors (Centi et al., 2007; Noemí et al., 2007; Golub et al., 2009; Hu et al., 2009). They have unique properties such as high specificity, low expense, small size, easy chemical modification, and more importantly remarkable flexibility, along with the fact that their design is not time consuming at all. In recent years, a variety of techniques such as surface plasmon resonance (Ohsawa et al., 2008; Tombelli et al., 2005; Wang et al., 2009), optical techniques (Huang et al., 2009; Li and Ho, 2008; Pavlov et al., 2005; Li et al., 2009), quartz crystal microbalance (Yao et al., 2009) and electrochemical techniques (Han et al., 2009; Hianik and Wang, 2009; Elbaz and Willner, 2009; Mir et al., 2008; Sassolas et al., 2009) have been applied for aptamer-based biosensors.

The significant advantages of electrochemical aptasensors such as their high sensitivity, simplicity, rapid response, reusability, and low cost, make them interesting sensors for the detection of various small molecules and proteins (Mascini, 2008) as well. The electrochemical methods are based on either redox indicators or label-free detections. Most of the redox based methods involve tedious modification or immobilization techniques. Furthermore, they are time consuming, cost-intensive, and more importantly they may affect the affinity of the aptamer. Therefore, the development of label-free aptasensors is a promising strategy. Substantial efforts have been devoted to the development of label-free aptasensors based on electrochemical impedance spectroscopy (EIS) (Radi et al., 2005; Katz and Willner, 2003; Rodriguez et al., 2005). EIS is a powerful method for characterizing biomolecule-functionalized electrodes, and also for monitoring biorecognition events that occur on the electrode surfaces (Katz and Willner, 2003). EIS is a nondestructive technique that makes it extremely attractive for electrochemical biosensing assays (Radi et al., 2005; Elbaz et al., 2008; Rodriguez et al., 2005; Zayats et al., 2006).

* Corresponding author. Tel.: +98 311 793271; fax: +98 311 6689732.
E-mail address: m.mehrgardi@chem.ui.ac.ir (M.A. Mehrgardi).

0956-5663/$ – see front matter © 2012 Elsevier B.V. All rights reserved.
doi:10.1016/j.bios.2011.12.050

A label free electrochemical aptasensor for the detection of DCF is described in this paper. DCF is one of the most common drugs that has been used over the years. It is a non-steroidal drug (NSAID) with analgesic, anti-inflammatory, and antipyretic properties (Nokhodchi et al., 2007). In order to construct the biosensor, amino-labeled aptamer is immobilized on the surface of a glassy carbon electrode. The immobilization of aptamer on the surface of GCE and the loading of DCF on the aptamer were monitored using voltammetric and EIS techniques.

In order to support the electrochemical experiments, the present paper investigates the changes in the plasmonic band of silver nanoparticles (Ag-NPs) upon the modification with the aptamer and DCF. Metal nanoparticles (NPs) have unique physical, chemical, and electronic properties which generate a frenzy of excitement. "Solutions and solids containing metal NPs of gold, silver, or copper feature beautiful bright colors due to a physical property called the surface plasmon band (SPB)" (Moores and Le Floch, 2009). Ag-NPs offer super strong light scattering at their plasmon resonance frequency without any photobleaching (Jain et al., 2008).

2. Experimental

2.1. Chemicals

Silver nitrate, sodium borohydride, trisodium citrate, sodium dihydrogen phosphate, disodium hydrogen phosphate, sodium chloride, 1-ethyl-3-(3-dimethylaminopropyl) carbodiimide hydrochloride (EDC), N-hydroxysuccinimide (NHS) and 6-aminohexanoic acid (AHA) were purchased from Merck in analytical grade and were used as received. Sodium diclofenac was received from Exir pharmaceutical company (Iran) as a gift. The following amino-functionalized aptamer (OD = 20) which has been designed for specific detection of DCF and was previously reported by Joeng et al. (2009) was obtained from Eurofins-MWG-Operon:

3′NHC$_7$ATACCAGCTTATTCAATTGCAACGTGGCGGTCAGTCAGC-GGGTGGTGGGTTCGGTCCAGATAGTAAGTGCAATCT-5′.

The aptamer was received as a lyophilized powder and was then dissolved in 5.00 mL salinated phosphate buffer (PBS) pH 7.4 containing 0.01 M Na_2HPO_4, 0.002 M KH_2PO_4, 0.15 M NaCl and 0.15 M KCl. Serum samples of healthy human volunteer blood donations were obtained from Esfahan Blood Transfusion Organization (EBTO). All the solutions used throughout the work were prepared using deionized doubly distilled water (18 MΩ cm^{-1} resistivity) from a Millipore system.

2.2. Instrumental

All electrochemical measurements were carried out using an Autolab PGSTAT30 (ECOchemie, The Netherlands, driven by GPES 4.9 software). A conventional three electrodes configuration consisting of the modified glassy carbon as the working electrode (2 mm in diameter, Azar electrode Inc.), an Ag/AgCl/3 M KCl as a reference electrode, and a platinum wire as an auxiliary electrode was used. The impedance measurements were performed in the presence of a $K_3[Fe(CN)_6]/K_4[Fe(CN)_6$ (1:1, 0.5 mM) mixture, in a solution that contained KCl (0.15 M) and NaCl (0.15 M). They were recorded by applying a potential equal to that of the open circuit (OCP), 0.23 V (vs. Ag/AgCl), the oscillation potential of 5.0 mV over the frequency range of 10 kHz to 0.1 Hz. The SPB measurements were performed using a JASCOV-670 UV–Vis. spectrophotometer.

2.3. Fabrication of aptamer-based electrochemical sensor

Scheme 1 illustrates various steps of fabrication of aptamer-based electrochemical sensor. Glassy carbon electrode was sequentially polished using 1.0, 0.3 and 0.05 μm α-alumina slurry.

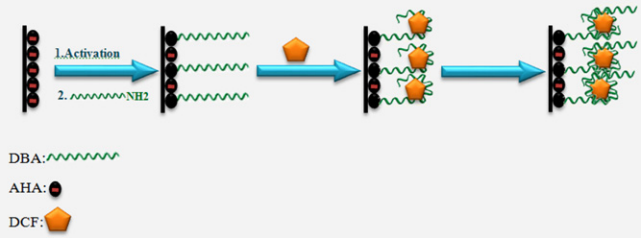

Scheme 1. Schematic presentation of different steps of biosensor construction.

It was then sonicated for 5 min in ethanol and water respectively. When the surface was cleaned, the glassy carbon electrode was oxidized at 0.5 V for 1 min in PBS solution (pH 7.4) and it was rinsed. The generated carboxylic acid groups on the surface of GCE were activated by immersing in a solution containing 5 mM EDC and 8 mM NHS in 1X PBS buffer for 1 h. AHA was covalently attached to the activated carboxylic groups as a result of dropping 20 μL of 10 mM AHA on the oxidized surface of GCE and placing it under radiation of the microwave for 5 min to form carbodiimide bond (GCE/AHA). Then the electrode was rinsed with the buffer solution. Again, the terminal carboxylic acid groups of AHA were activated by immersing in the PBS solution (pH 7.4) containing 5 mM EDC and 8 mM NHS for 1 h. The electrode was then thoroughly rinsed with the buffer solution.

The aptamer modified electrode was prepared by dropping 20 μL of 1.3 μM amino labeled aptamer solution on the resulting electrode held upside-down (GCE/AHA/DBA). Afterwards, the end of the electrode was covered with a plastic cap to protect the solution from evaporation. This modified electrode was kept for 20 h at 4 °C. Prior to use, the modified electrode was rinsed with 1X PBS buffer for a couple of minutes. The modified electrode was incubated in various concentrations of DCF for 2 h (GCE/AHA/DBA/DCF). To remove nonspecific adsorption of DCF, the electrode was then rinsed with PBS buffer after incubated in DCF. Finally, another 20 μL aliquot of 1.3 μM amino labeled DBA solution was dropped on the electrode which was held upside-down to complete the sandwich format assay (GCE/AHA/DBA/DCF/DBA). At last step, to remove the nonspecific adsorbed secondary DBA, the modified electrode was rinsed with PBS buffer. Each step of modifications has been followed using CV and EIS experiments.

For the determination of DCF in a blood serum sample, a stock solution of 1 mM DCF in human serum was prepared, and then it was diluted using PBS buffer (pH 7.4) to obtain 10.0, 14.0, and 20.0 μM DCF solutions and finally, they were analyzed by the proposed aptasensor.

2.4. Synthesis of silver nanoparticles (Ag-NPs)

Ag-NPs were synthesized according to the procedure previously described in the literature (Mulfinger et al., 2007). Briefly, a large excess amount of sodium borohydride is necessary both to reduce the ionic silver and to stabilize the silver nanoparticles. 5.00 mL silver nitrate (1.0 mM) was added drop by drop to 15.0 mL of 2.0 mM ice-cold sodium borohydride solution (~1 drop/s). The reaction mixture was stirred vigorously on a magnetic stirrer. The solution turned to light yellow after the addition of 2.0 mL of silver nitrate and later turned to brighter yellow when more silver nitrate was added. Finally, in order to minimize the aggregation of Ag-NPs, 0.06 g tri-sodium citrate was added to the resulting solution.

The sizes of the Ag-NPs were verified using transmission electron microscopy (TEM) analysis (Zeiss, EM 900). It was equal to 10 ± 3 nm as is shown in Fig. 4A.

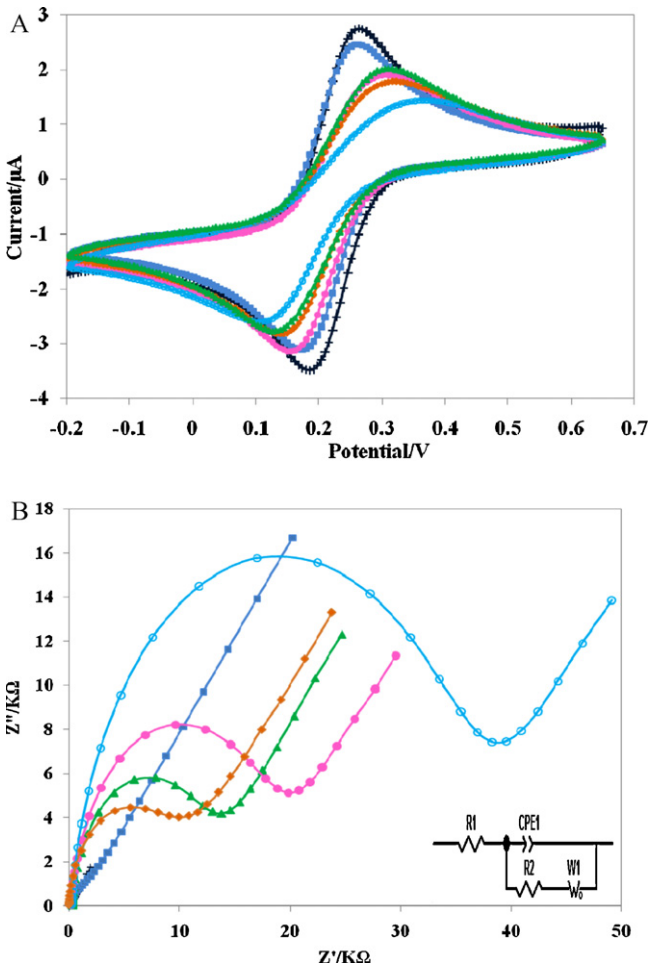

Fig. 1. Characterization of the sensing interface by (A) CV and (B) EIS: Bare GCE (+), GCE/AHA (■) GCE/AHA/DBA (▲), GCE/AHA/DBA/1 μM DCF (●), GCE/AHA/DBA/5 μM DCF (○) and GCE/AHA/DBA/500 μM DCF (♦).

2.5. Preparation of Ag-NPs/DBA probes for plasmonic investigations

The aptamer-adapted silver nanoparticles (Ag-NPs/DBA) for the plasmonic investigation were prepared as is followed: First, the citrate layer on the surface of 250 μL Ag-NPs was activated by dropping 50 μL of the solution containing 5 mM EDC and 8 mM NHS in 1X PBS buffer (pH 7.4) for 1 h. The amino labeled DBA was then covalently bound to the activated carboxylic groups on the surface of Ag-NPs by adding 50 μL of 1.3 μM DBA to the activated Ag-NPs solution for 1 h. This assembly (Ag-NPs/DBA) was then imposed to 50 μL DCF solution for 1 h. Finally, functionalization with the secondary DBA was done by dropping 50 μL of the secondary DBA into this solution.

3. Results and discussion

3.1. Electrochemical characterization of the modified electrode

The changes in the characteristics of the surface of GCE by electrochemical oxidation and also the modification with AHA, DBA, DCF and the secondary DBA could be monitored using both CV and EIS techniques. Fig. 1A shows the voltammograms of 5.0×10^{-4} M ferrocyanide ion on the bare GCE, GCE/AHA, GCE/AHA/DBA and GCE/AHA/DBA/DCF at various concentrations of DCF. By immobilizing AHA on the surface of the oxidized GCE, the negative charges on the surface of the electrode are developed in neutral pHs. Consequently, the diffusion of ferrocyanide ion to the electrode surface is rarely blocked. Upon the immobilization of DBA on GCE/AHA, the phosphate backbone of the DBA develops more negative charges on the GCE surface. The negatively charged interface repels the negative redox probes, $[Fe(CN)_6]^{3-/4-}$ anions. This repulsion causes a decrease in the interfacial electron-transfer rate of the probes (Radi et al., 2005). Due to these events, the peak currents are significantly decreased. Moreover, the peak potential separations (ΔEp) are increased compared to that of the bare electrode. The addition of DCF, up to 5 μM, slightly increases the charge transfer resistance of the surface. However, at higher concentrations of DCF, the resistance is decreased suggesting the conformation changes in the DBA. Fig. 1B shows the impedance spectra for the assay under these conditions.

3.2. Quantitation of surface density of aptamer immobilization

The coverage of DNA (aptamer) immobilization on the electrode surface can be estimated using the number of cationic redox molecules that electrostatically associated to the anionic phosphate backbone of DNA (Steel et al., 1998). Briefly, after the immobilization of aptamer on the electrode surface, the modified electrode was placed in ruthenium (III) hexaamine (RuHex) solution with low ionic strength (0.05 M KCl). Then the amount of cationic redox marker, RuHex, was measured by chronocoulometry technique. Using the Cottrell equation, the chronocoulometric intercept at $t = 0$ is summation of the double layer charging and surface terms. The surface surplus terms are determined by the difference between the chronocoulometric intercepts for the identical potential step experiment in the presence and absence of redox marker. By following the relationship of the saturated surface surplus of RuHex in converted to DNA surface density.

$$\Gamma_{apt} = \Gamma^0 \left(\frac{z}{m}\right)$$

where Γ_{apt} is the probe surface density in molecules/cm^2, m is the number of bases in aptamer, z is the charge of RuHex. At last the surface density of probe DNA has been obtained equal to 40 pmol cm^{-2}.

3.3. Analytical characteristics of GCE/AHA/DBA electrode for DCF determination

Fig. 2A depicts the cyclic voltammograms of GCE/AHA/DBA after incubation of this electrode in the different concentrations of DCF, over a range of 0–5 μM and subsequently, dropping of 20 μL of secondary DBA (1.3 μM) on the surface of GCE/AHA/DBA/DCF. By increasing the concentration of DCF up to 5 μM, the currents are significantly decreased and the peak potential separations (ΔEp) are increased.

EIS complex plane plots also obtained under the same conditions (Fig. 2B). The plot of $(R_{ct_i} - R_{ct_0})$ versus the concentration of DCF is linear over 0–5.0 μM (inset plot of Fig. 2B, $[\Delta R_{ct}\,(k\Omega) = 14.26\,k\Omega\,C_{DCF}/\mu M + 15.66\,k\Omega$, $R^2 = 0.998]$), where R_{ct_0} and R_{ct_i} refer to the charge transfer resistance of GCE/AHA and GCE/AHA/DBA/DCF/DBA, respectively. The detection limit of 2.7×10^{-7} M DCF was estimated based on $3s_b$. The sensitivity of the biosensor toward DCF in impedimetric measurement was 15.66 kΩ μM^{-1} at concentration range up to 5 μM. As the figure shows, by increasing the concentrations of DCF up to 5 μM, the interfacial charge transfers resistances are increased. It is demonstrated that by increasing the concentrations of DCF, more sites of DBA are occupied by DCF molecules. Consequently, more secondary aptamers are accumulated on the surface of the electrode. At ~5 μM DCF, all of DBA sites on the surface are occupied by DCF molecules.

By the way, higher concentrations of DCF cause some changes in the spatial conformation of DBA and do not bring more

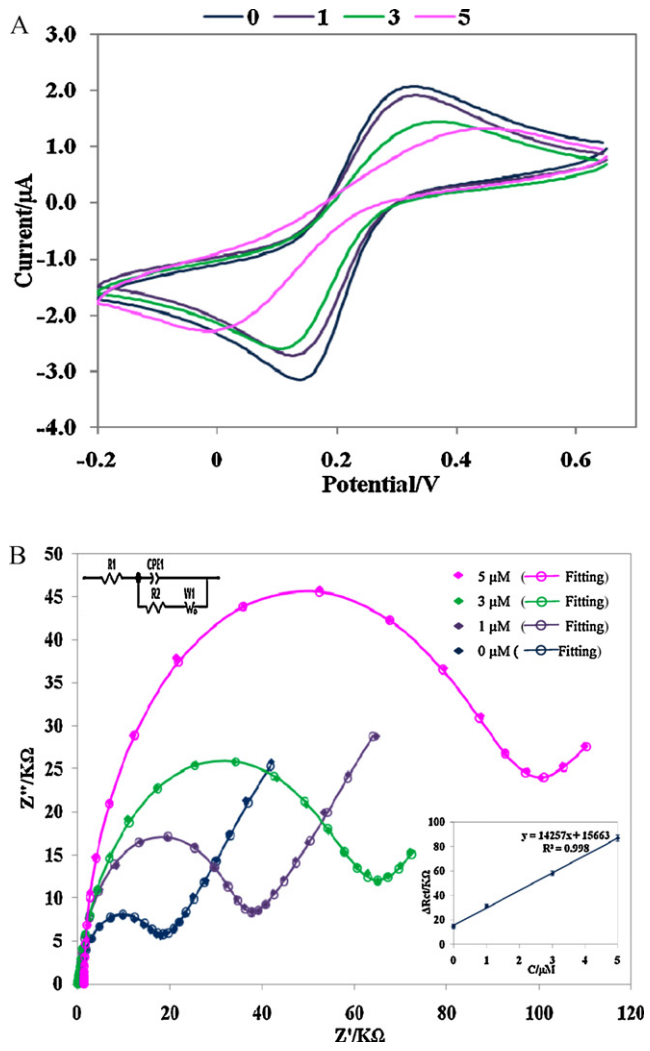

Fig. 2. (A) Cyclic voltammograms, and (B) the EIS complex plane plots obtained in the presence of 5.0×10^{-4} M $[Fe(CN)_6]^{3-/4-}$ as a redox probe, after treatment of the GCE/AHA/DBA complex with different concentrations of DCF: 0 μM (blue), 1 μM (violet), 3 μM (green), 5 μM (pink) and with secondary DBA. Solid lines with empty symbols indicate corresponding fitting results. Inset indicates the modified Randles' equivalent circuit model for the impedance spectra. Inset plot shows the dependence of ΔR_{ct} on the concentration of DCF. $\Delta R_{ct} = (R_{ct_i} - R_{ct_0})$, where R_{ct_0} and R_{ct_i} refer to the electron transfer resistance of GCE/AHA and GCE/AHA/DBA after incubation with the varying concentrations of DCF and with secondary DBA, respectively. The error bars indicate the standard deviation of three successive measurements for each concentration. (For interpretation of the references to color in this figure legend, the reader is referred to the web version of the article.)

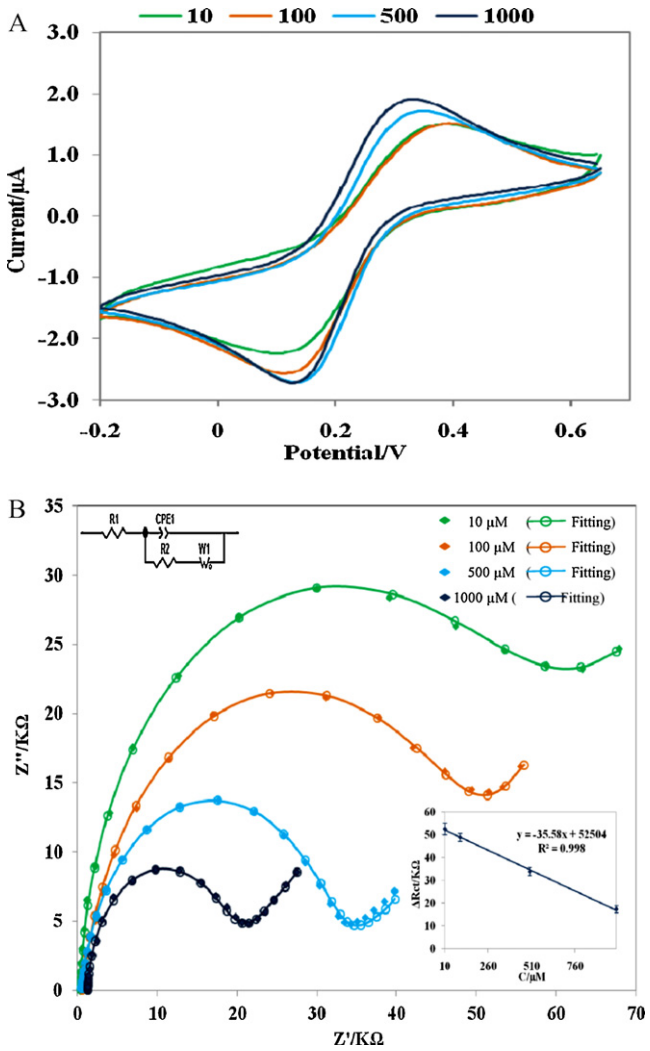

Fig. 3. (A) Cyclic voltammograms, and (B) the EIS complex plane plots obtained in the presence of 5.0×10^{-4} M $[Fe(CN)_6]^{3-/4-}$ as a redox probe, after treatment of the GCE/AHA/DBA complex with different concentrations of DCF: 10 μM (green), 100 μM (orange), 500 μM (light blue), 1000 μM (dark blue) and with secondary DBA. Solid lines with empty symbols indicate corresponding fitting results. Inset circuit model indicates the modified Randles' equivalent circuit model for the impedance spectra. Inset plot shows the dependence of ΔR_{ct} on the concentration of DCF. $\Delta R_{ct} = (R_{ct_i} - R_{ct_0})$, where R_{ct_0} and R_{ct_i} refer to the electron transfer resistance of GCE/AHA and GCE/AHA/DBA after incubation with the varying concentrations of DCF and with secondary DBA, respectively. The error bars indicate the standard deviation of three successive measurements for each concentration. (For interpretation of the references to color in this figure legend, the reader is referred to the web version of the article.)

secondary aptamer on the surface. The results demonstrate that these conformational changes lower the negative charge density on the surface and therefore, it causes an increase in the peak currents of the voltammograms of potassium ferricyanide on GCE/AHA/DBA/DCF/DBA at the concentrations of DCF over than 5 μM up to 1000 μM (Fig. 3A). Moreover, these conformational changes decrease the interfacial charge transfer resistance to the negatively charged redox probe, $[Fe(CN)_6]^{4-/3-}$, as compared to the primary conformation of the aptamer in the lower concentrations of DCF (Fig. 3B).

3.4. Reproducibility, selectivity and stability of the aptasensor

In order to evaluate the inter-day variations of the aptasensor, a series of three electrodes was examined for the detection of 10 μM DCF. The relative standard deviation (RSD) of 4.7% for these measurements has been obtained. This shows the reproducibility of the aptasensor is quite reliable.

In order to examine the ability of this aptasensor for the determination of DCF in real samples, control experiments were carried out in both the standard solution and the diluted serum sample. Maximum levels of DCF in human blood serum are achieved from 1 to 4 h after oral administration. Average concentration of drug in serum is ~4000 ng mL^{-1} (13.5 μM) (Lill et al., 2000).

As shown in Table 1, the R_{ct} values for both cases almost remained unchanged. This implies that the label-free aptasen-

Table 1
Determination of DCF in a blood serum sample.

C_{DCF} (μM)$_{added}$	C_{DCF} (μM)$_{founded}$	Recovery%
10	10.3	103.0
14	14.2	101.4
20	19.8	99.0

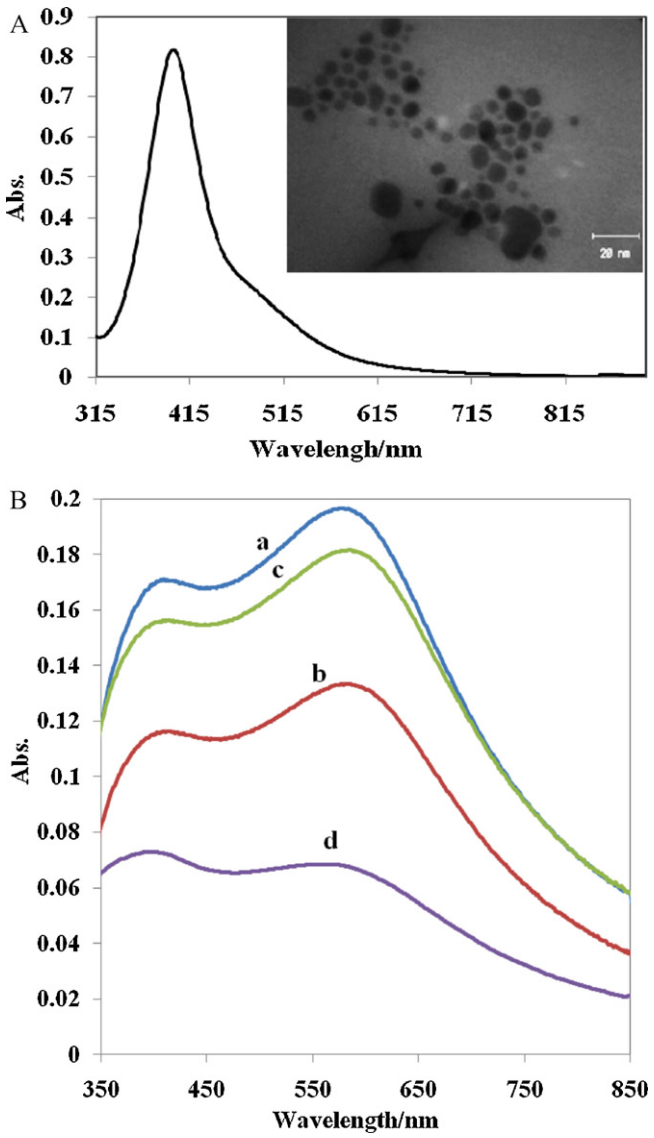

Fig. 4. (A) Absorption spectrum of Ag NPs and TEM image of Ag–NPs (inset plot). (B) Absorption spectra of SNP/EDC/NHS (a), SNP/EDC/NHS/DBA (b), SNP/EDC/NHS/DBA/DCF (c) and SNP/EDC/NHS/DBA/DCF/DBA (d) respectively, with their corresponding characteristic absorption peaks at 410, 408, 415, and 396 nm.

sor has a promising perspective for the analytical application in complex biological matrixes. The stability of the aptasensor was examined by storing the sensor in PBS solution (pH 7.4) at 4 °C. After 5 days, a decrease of 3% was observed for the detection of the same DCF concentration, implying good electrode stability.

3.5. Plasmonic investigations

Ag-NPs have unique properties, such as low cost, easy stabilization and simple functionalization as well. The SPB phenomenon is responsible for the bright color of the solutions containing Ag-NPs (Merkoçi, 2009). Under photoexcitation, the conduction electrons of the nanoparticle oscillate collectively, which causes a strong absorption band in the visible region of the spectrum. These properties, especially the plasmonic characteristics of Ag-NPs, make them very promising probes for the sensing purposes. Here, the aptamer-adapted silver nanoparticles (Ag-NPs/DBA) are used as an optical probe to confirm aptamer–DCF interaction, wherein Ag-NPs act as the illuminophores and the aptamer acts as a recognition element.

Ag-NPs, with an average size of 10 ± 3 nm, show a strong absorption band in the visible region as is shown in Fig. 4A. Amino-labeled DBA was covalently bound to the citrate groups on the surfaces of the nanoparticles through EDC/NHS chemistry. Subsequently, Ag-NPs/DBA was incubated with the DCF solution and finally functionalization with the secondary DBA was done. All of these steps could be monitored by the changes in the plasmonic band of Ag-NPs. The representative UV/vis spectra for activated Ag-NP by EDC/NHS, and Ag-NPs/DBA, Ag-NPs/DBA/DCF and Ag-NPs/DBA/DCF/DBA are shown in Fig. 4B. The comparison between the spectrum of Ag-NPs in Fig. 4A with the spectrum of activated nanoparticles in Fig. 4B shows that the peak in 400 nm decreases significantly, and a new shoulder is appeared at so longer wave lengths (roughly around 580 nm). Furthermore, the color changes could be easily seen by bare eyes. It could be due to aggregation of some nanoparticles by diminishing of the negative charges of the carboxylate groups that formed carbodiimide bond with EDC/NHS. Then, by immobilizing the aptamers on the surface of nanoparticles, the absorption is decreased again. The Ag-NPs/DBA was then treated with DCF to obtain Ag-NPs/DBA/DCF format. Due to the changes in the conformation of the DBA, hyperchromicity effect occurs in the absorption spectrum, which is in consistency with the electrochemical observations. At the last step, the sandwich assay (Ag-NPs/DBA/DCF/DBA) is formed by incubation of Ag-NPs/DBA/DCF with the secondary DBA solution. This causes the hypochromic effect, and the absorption is strongly decreased.

4. Conclusion

A label free electrochemical aptasensor for the determination of sodium diclofenac has been introduced in this manuscript. Sodium diclofenac was sandwiched between two aptamers on the surface of a glassy carbon electrode. The blocking of $[Fe(CN)_6]^{3-/4-}$ as a negative probe to the surface by the negatively charged aptamer could retard the electron-transfer kinetics of the redox probe. These phenomena were followed using voltammetric and EIS techniques. The calibration curve of biosensor shows two different linear ranges over 0–5 μM and 10–1000 μM. A detection limit of 2.70×10^{-7} M and sensitivity 15.66 kΩ μM^{-1} and RSD mean of 4.7%was obtained. The validity of the method and applicability of the aptasensor were successfully investigated by the determination of DCF concentration in a human blood serum sample. Furthermore, the changes in the plasmonic band of Ag-NPs upon the modification with the aptamer and DCF have been investigated. The results are in line with the electrochemical experiments.

Acknowledgments

The authors gratefully appreciate the financial support of this project by the research council of the University of Isfahan. We like also to express sincere thanks to Miss. Rayehe Sattarinezhad, for her careful editing of the manuscript. Also we would like to express our sincere acknowledgements to Exir pharmaceutical company for offering us sodium diclofenac as a gift and Esfahan Blood Transfusion Organization (EBTO) providing serum samples of healthy human volunteer blood donations.

References

Centi, S., Tombelli, S., Minunni, M., Mascini, M., 2007. Anal. Chem. 79 (4), 1466–1473.
Elbaz, J., Shlyahovsky, B., Gill, R., Li, D., Willner, I., 2008. ChemBioChem 9, 232–239.
Ellington, A.D., Szostak, J.W., 1990. Nature 346, 818–822.
Golub, E., Pelossof, G., Freeman, R., Zhang, H., Willner, I., 2009. Anal. Chem. 81 (22), 9291–9298.
Han, K., Chen, L., Lin, Z., Li, G., 2009. Electrochem. Commun. 11 (1), 157–160.
Hianik, T., Wang, J., 2009. Electroanalysis 21 (11), 1223–1235.
Hu, L., Bian, Z., Li, H., Han, S., Yuan, Y., Gao, L., Xu, G., 2009. Anal. Chem. 81 (23), 9807–9811.

Huang, H., Jie, G., Cui, R., Zhu, J.-J., 2009. Electrochem. Commun. 11 (4), 816–818.
Elbaz, J., Moshe, M., Willner, I., 2009. Angew. Chem. Int. Ed. Engl. 48, 3834.
Jain, P.K., Huang, X., El-Sayed, I.H., El-Sayed, M.A., 2008. Acc. Chem. Res. 41 (12), 1578–1586.
Joeng, C.B., Niazi, J.H., Lee, S.J., Gu, M.B., 2009. Bioorg. Med. Chem. 17, 5380–5387.
Katz, E., Willner, I., 2003. Electroanalysis 15 (11), 913–947.
Li, N., Ho, C.-M., 2008. J. Am. Chem. Soc. 130 (8), 2380–2381.
Li, T., Shi, L.L., Wang, E.K., Dong, S.J., 2009. Chem. Eur. J. 15, 1036–1042.
Lill, J.S., O'Sullivan, T., Bauer, L.A., Horn, J.R., Carithers, R., Strandness, D.E., Lau, H., Chan, K., Thakker, K., 2000. J. Clin. Pharmacol. 40, 250–257.
Mascini, M., 2008. Aptamers in Bioanalysis. Wiley-Blackwell, Oxford.
Merkoçi, A., 2009. Biosensing Using Nanomaterials. Wiley, Hoboken.
Mir, M., Jenkins, A.T.A., Katakis, I., 2008. Electrochem. Commun. 10 (10), 1533–1536.
Moores, A., Le Floch, P., 2009. The Metal Nanoparticle Plasmon Band as a Powerful Tool for Chemo- and Biosensing. John Wiley & Sons, Inc.
Mulfinger, L., Solomon, S.D., Bahadory, M., Jeyarajasingam, A.V., Rutkowsky, S.A., Boritz, C., 2007. J. Chem. Educ. 84 (2), 322.
Nokhodchi, A., Sharabiani, K., Rashidi, M.R., Ghafourian, T., 2007. Int. J. Pharm. 335, 97–105.
Noemí, D.-L.-S.-Á., Lobo-Castañón, M.J., Miranda-Ordieres, A.J., Tuñón-Blanco, P., 2007. J. Am. Chem. Soc. 129 (13), 3808–3809.
Ohsawa, K., Kasamatsu, T., Nagashima, J.I., Hanawa, K., Kuwahara, M., Ozaki, H., Sawai, H., 2008. Anal. Sci. 24 (1), 167–172.
Pavlov, V., Shlyahovsky, B., Willner, I., 2005. J. Am. Chem. Soc. 127 (18), 6522–6523.
Radi, A.-E., Sanchez, J.L.A., Baldrich, E., O'Sullivan, C.K., 2005. Anal. Chem. 77, 6320–6323.
Roberston, D.L., Joyce, G.F., 1990. Nature 344 (344), 467–468.
Rodriguez, M.C., Kawde, A.-N., Wang, J., 2005. Chem. Commun. (34), 4267–4269.
Sassolas, A., Blum, L., Leca-Bouvier, B., 2009. Electroanalysis 21 (11), 1237–1250.
Steel, A.B., Herne, T.M., Tarlov, M.J., 1998. Anal. Chem. 70, 4670–4677.
Tombelli, S., Minunni, M., Luzi, E., Mascini, M., 2005. Bioelectrochemistry 67 (2), 135–141.
Tuerk, C., Gold, L., 1990. Science 249, 505–510.
Wang, J., Munir, A., Zhou, H.S., 2009. Talanta 79 (1), 72–76.
Yao, C., Qi, Y., Zhao, Y., Xiang, Y., Chen, Q., Fu, W., 2009. Biosens. Bioelectron. 24 (8), 2499–2503.
Zayats, M., Huang, Y., Gill, R., Ma, C.-a., Willner, I., 2006. J. Am. Chem. Soc. 128 (42), 13666–13667.